EUROPEAN ORGANIZATION FOR NUCLEAR RESEARCH
ORGANISATION EUROPEENNE POUR LA RECHERCHE NUCLEAIRE

CERN PS DIVISION

CERN PS 2001-065(BD)

N_2 and Xe Gas Scintillation Cross-Section, Spectrum, and Lifetime Measurements from 50 MeV to 26 GeV at the CERN PS and Booster

J. Bosser[1], E. Bravin[1], R. Maccaferri[1], M.A. Plum[2]

Abstract

Beam parameters in CERN's Proton Synchrotron (PS) accelerator must be controlled (and measured) with tighter precision than ever before to meet the stringent requirements of the Large Hadron Collider (LHC) programme. A non-destructive beam profile measurement system would be a valuable diagnostic tool. To this end, we measured N_2 and Xe gas scintillation absolute cross-sections and lifetimes for proton beam energies from 1.4 to 25 GeV, which should prove valuable in the design and construction of a gas scintillation profile measurement system. We also measured relative cross-sections for proton beam energies between 0.05 and 1.4 GeV.

(To be submitted to Nuclear Instruments and Methods)

Geneva, Switzerland
28 November 2001

1) European Organization for Nuclear Research (CERN), CH-1211 Geneva 23, Switzerland
2) Present address: Los Alamos National Laboratory (LANL), Los Alamos, N.M. 87454, USA

Introduction

Beam parameters in CERN's Proton Synchrotron (PS) accelerator must be controlled (and measured) with tighter precision than ever before to meet the stringent requirements of the Large Hadron Collider (LHC) programme. For example, it could be desirable to measure transverse profiles continuously throughout the acceleration cycle, and to do this, a non-destructive beam profile measurement system is necessary. We considered several different technologies for making such a measurement, including inverse laser Compton scattering, residual gas ionization, and gas scintillation. Given the constraints of technical feasibility and available space in the PS, we determined that our best option was a system based on measuring light from gas scintillation.

In a gas scintillation profile monitor, gas molecules in the beam pipe, from either residual or injected gas, are excited by the passing particle beam. The molecules may or may not be ionized, but in any case electrons are promoted to excited states. When the electrons fall to lower energy orbits, photons are emitted. If the molecules have not traveled too far from the points where the interactions with the particle beam took place, the photons can be collected to produce an accurate measure of the beam profile. If the emission lines are in the visible spectrum, simple glass lenses can be used to focus the light onto detectors. The perfect gas would have large cross-sections in the visible region and short excited-state lifetimes. If gas injection into the beam pipe is necessary, the gas should also be easily pumped by the vacuum system.

Cross-section measurements found in literature [1],[2] on N_2 at 200 keV incident proton energy showed strong lines from the N_2^+ system at 391.4 and 427.8 nm, along with several weaker lines also in the visible range. Other investigators [3] measured the lifetimes of these states to be about 60 ns. Also, most vacuum systems efficiently pump N_2 gas. This makes N_2 a useful gas for profile measurements. However, the proton energy range for our application is 1.4 to 25 GeV – far above the 200 keV measurements. Other investigators [4],[5],[6],[7] have made rough measurements of N_2 gas cross-sections and lifetimes at energies closer to our range of interest, but the various measurements do not seem to be consistent, in terms of either the cross-sections or the lifetimes.

Measurements made with Xe gas suggest that this could also be a good gas for a profile monitor. The light production cross-sections are large in the visible range, and some of the lifetimes are short [8]. This gas is also easily pumped by vacuum systems. However, even less work has been done with Xe than with N_2. In view of the lack of accurate measurements on N_2 at proton energies in our range of interest, and an even shorter supply of Xe data, we decided to embark on a series of measurements of the N_2 and Xe cross-sections and lifetimes at the CERN PS and Booster Synchrotrons.

Experimental Setup in the PS machine

A vacuum tank was built and installed just downstream of magnet 100, in section 1, of the PS synchrotron. This location, despite its non-optimal background radiation conditions, is the only location in the machine with sufficient space for the installation. The interior of the tank is blackened with chromium-oxide to minimize light reflections, and a quartz vacuum window on one side of the tank allows light from gas scintillation to be measured. A port on the opposite side allows gas to be injected into the tank through a remote-controlled leak valve. A Penning vacuum gauge is mounted on a port below the tank to measure the vacuum pressure. The gas injection system has been tested up to 0.013 Pa (10^{-4} torr) N_2 gas without affecting any measurable proton or lepton beam parameters. However, when the PS is accelerating partially-stripped ions on other beam cycles, even the slightest additional gas pressure is too much. Two different gases may be injected with the system, and for our measurements we chose N_2 and Xe.

To minimize problems due to background radiation, we built an optical system to transmit the light to a photomultiplier tube (PMT) 4.6 m away, behind concrete shielding, as shown in Figure 1. Four lenses are supported inside a stainless steel pipe with vacuum windows on either end. The pipe is evacuated to a pressure less than 2.7 Pa (0.02 torr) to avoid the possibility of beam loss causing gas scintillation in the air inside the optical system. The vacuum window on the vacuum tank mounted in the PS, and the first vacuum window of the optical system, are made of radiation-hard quartz. The first optical lens in made of radiation-hard fused silica. The rest of the lenses are achromatic lenses made of ordinary optical glass. We used the commercially available ZEMAX [9] optical design computer code to optimize and characterize our optical system.

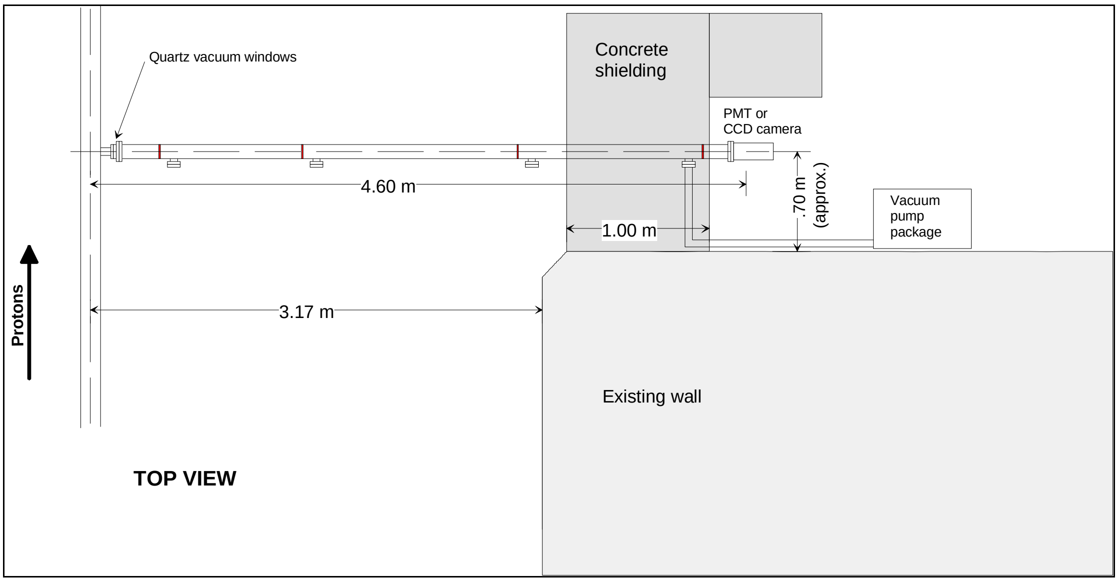

Figure 1. Optical system used in the PS.

The Philips XP2020 PMT is connected to a Phillips 6908 low level discriminator in a room beneath the accelerator. A serial-link computer-controlled power supply positioned near the low-level discriminator controls its threshold setting. The output of the low-level discriminator is connected to a CAMAC discriminator, then counted by a CAMAC scaler. A block diagram is shown in Figure 2. The low-level discriminator output may alternatively be connected to a time-to-analog converter to measure the excited state lifetimes. This option is discussed in more detail in the lifetime section.

When a photon strikes the PMT photocathode, a single electron is sometimes emitted, depending on the wavelength of the photon and the quantum efficiency of the photocathode. The single electron produces a pulse at the PMT anode of a certain amplitude, depending on the single electron spectrum (SES) of the PMT and its operating parameters. Our measurements showed that a discriminator setting of about 6 or 7 mV is optimal to separate the PMT noise from the single electron signal. With such a low threshold setting, it is important that the cable between the PMT and the discriminator is kept short so as not to smear out the signal, pick up electrical noise, and/or introduce ground loops. Tests with the PMT in the beam tunnel and the discriminator located near the control room (about 100 m cable length) showed that under these conditions the SES signal is too smeared out to make a good measurement. To avoid this effect we positioned the discriminator in the tunnel beneath the PS accelerator and used a short cable, about 10-m long, which allows us to easily resolve the SES.

Between the PMT and the exit of the optical system is a remote-controlled nine-position wheel containing various types of optical filters, for coarse spectral measurements, and blinds, for background measurements. The wheel position is remotely controlled from the control room.

The CAMAC modules are read out by a program running on the PS control system. The PMT counts can be measured during any beam cycle for any start and stop times. For each measurement, we also acquire the discriminator threshold, the beam intensity and the vacuum pressure. The user can perform measurements simultaneously on up to four different cycles within the PS supercycle. The data is then presented in a histogram for visual feedback of the ongoing operation as well as stored for further offline processing.

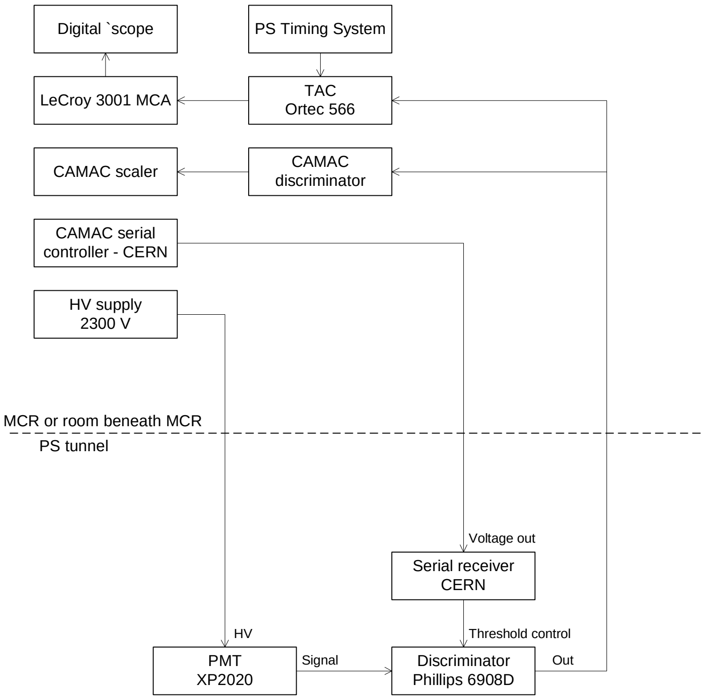

Figure 2. Block diagram of the electronics.

Experimental Setup in the Booster machine

In addition to the absolute cross-section measurements in the PS synchrotron, we also made relative cross-section measurements in the Booster synchrotron. The Booster accelerates protons from 0.05 to 1.4 GeV, which, for the case of a proton beam, covers an energy range corresponding to a sharply decreasing stopping power, or dE/dx. This measurement, although not absolute, thus represents a good test of the relationship between dE/dx and gas scintillation cross-sections.

For this measurement an EG&G C-942 channel PMT was mounted on an available optical port with a sapphire window in Section 12 of Ring 1. Like the XP2020 used in the PS experiments, the C-942 is capable of counting single photon events. A remote-controlled optical blind could be rotated into place directly in front of the PMT to allow background measurements. With the Booster gas system we could only inject a single gas species, and we chose N_2. A low-level discriminator, set for a threshold of 15 mV, was located in the Booster control room. The signal to noise ratio was quite good – typically better than 100. Our data are shown in Table 1.

Table 1. Booster signal levels, normalized to the 1.4 GeV (2.1 GeV/c) measurement

Momentum (GeV/c)	Normalized counts
0.32	6.0
0.56	2.6
2.1	1.0

Data analysis - background subtraction

In our experiment there are four signal sources due to photons and three non-photon sources such as protons and neutrons striking the PMT, as shown in Table 2.

Table 2. Signal sources.

Photons	Other
Gas scintillation (P_s)	Activation (S_a)
Background light (P_b)	Gas-induced beam loss (S_g)
Activation (P_a)	PMT background counts (S_d)
Gas-related beam loss (P_g)	

The gas scintillation photons, P_s, are the photons we seek to count to measure the gas scintillation cross-section. All other signal sources are backgrounds that must be subtracted.

The background light photons, P_b, come from light inside the PS ring. Sources include hot filaments of ionization gauges, vacuum windows, etc.

The activation photons, P_a, come from gas scintillation caused by radio activation of beam-line elements.

The gas-related beam loss photons, P_g, come from gas scintillation caused by gas-related beam loss. We are unable to separate this contribution to our measurement, since it is so similar to the gas scintillation signal we seek to measure. This component represents an inherent inaccuracy in our measurement. We have tested the magnitude of this contribution by purposely introducing beam loss, and we have concluded that it is smaller than other error sources in our measurement.

The activation signal, S_a, arises from beam line activation due to beam loss.

The gas-induced beam loss, S_g, comes from beam scattering off the gas we inject into the vacuum chamber.

The PMT background count photons, S_d, are the dark counts due to thermal electron emission from the PMT photocathode.

By making measurements with the beam on and off, the gas on and off, and the optical shutter open and closed, we can separate the various contributions to the background and subtract them from the gas scintillation signal. Four measurements are adequate for our purposes: the number of counts measured for 1) beam on, gas on, shutter open (*BGO*), 2) beam on, gas on, shutter closed (*BGC*), 3) beam on, gas off, shutter open (*BNO*), and 4) beam on, gas off, shutter closed (*BNC*). The contributions to the signals are as follows:

$$BGO = P_s + P_b + P_a + P_g + S_a + S_g + S_d,$$

$$BGC = S_a + S_g + S_d\ ,$$

$$BNO = P_b + P_a + S_a + S_d\ ,$$

$$BNC = S_a + S_d.$$

The P_g contribution is negligible, so the combination

$$P_s = (BGO - BGC) - (BNO - BNC)$$

serves to isolate the contribution due to gas scintillation, and allows us to proceed with the cross-section calculation. We also made measurements with the beam off, shutter open and closed, and gas on and off, to check for consistency within our data set and improve our understanding of background contributions. To illustrate the magnitude of the background contributions, some representative samples from our data set are shown in Table 6. The background accounts for 12 to 26% of the total signal, depending on the beam momentum.

The background in the Booster was much better than the PS measurements, so no background corrections are necessary here. The true signal was typically more than 100 times greater than the background. Our results, normalized to the 2.1 GeV/c data point, are shown in Table 1.

Data analysis – cross-section calculation

To determine absolute cross-sections, the properties of the optical system must be accurately known. The experimental setup used for the PS measurements was designed with this in mind. Due to the mentioned relative nature of the Booster measurements, the following discussion pertains to the PS measurements only.

The cross-section can be calculated from our measurements using the relationship

$$n = \sigma \, \rho \, F \, L$$

where n = photon s^{-1},
σ = cross-section [cm^2],
ρ = molecular density of gas [cm^{-3}],
F = proton flux [s^{-1}], and
L = active length of detector [cm].

The parameter n is computed from the relationship

$$C = n \; A \; k_1 \; k_2 \; k_3 \; T_{\text{int}} \; ,$$

where C = the number of counts measured by the PMT / discriminator,
A = the acceptance of the optical system,
k_1 = the correction factor for the quantum efficiency of the PMT,
k_2 = the correction factor for the non-zero discriminator threshold,
k_3 = the correction factor for transmission of light through the lens system, and
T_{int} = the time interval over which counts are collected.

The molecular gas density, ρ, is computed from the ideal gas formula. The gas temperature is about 293 °K, known with an accuracy of about one percent. We measure the gas pressure with a Penning Gauge installed on the vacuum tank on the side opposite the gas inlet, where there is no gas flow, to enhance the accuracy of the measurement. Prior to installation the Penning Gauge was calibrated in the lab against a spinning ball, for both N_2 and Xe gas. The pressure accuracy is estimated [10] to be about 3%. The overall accuracy of the gas density measurement is therefore about 4%. For the case of 1.3 x 10^{-4} Pa (1 x 10^{-6} torr), where many of our measurements were made, ρ = 3.3 x 10^{10} cm^{-3}.

The proton flux is given by $F = N / T_{rot}$, where N is the number of circulating protons and T_{rot} is the rotation period. A DC current transformer in the PS ring is used to measure N with an accuracy estimated [11] to be 1%. The counting time interval, T_{int}, is our most accurate parameter, and is known to an accuracy of much better than 1%. For our measurements N was typically about 1 x 10^{12}, and T_{rot} varied between 2.095 and 2.293 µs.

The number of counts C (usually collected in 100 ms) is typically several thousand. If 10,000 counts are collected in 100 ms, the count rate would be 100 kHz. This rate is comfortably within the specifications of our equipment. Of course the peak count rate can be higher than the average count rate. For excited state lifetimes of about 60 ns (see lifetime section below), and a worst case of a single beam bunch in the PS, the difference between the peak and the average count rates is a factor of 33. In any case, we check for a linear relationship between counts and gas pressure.

The correction factor for the PMT quantum efficiency, k_1, depends on the wavelength of the photon, the PMT window material, and the PMT photocathode material. The XP2020 PMT has a borosilicate window, a bialkaline photocathode, and a quantum efficiency of 25% at 400 nm. To accurately compute the correction factor, the wavelengths of the photons and their relative intensities must be known. We assume here that the wavelengths and relative intensities measured by the 200 keV proton experiment [2] found in literature are correct for our case, and take the PMT quantum efficiency vs. wavelength from the manufacturer's data. The parameters are summarized in Table 3. The ratio of the product column sum to the cross-section column sum gives $k_1 = 0.244$. Of course the accuracy of k_1 relies on the validity of the low-energy cross-section and wavelength measurements. A conservative estimate for the accuracy of k_1 is 25%.

Table 3. Table to compute the quantum efficiency factor, k_1.

Wavelength[a] (nm)	Cross-Section[a] (x 10^{-19} cm^2)	PMT quantum efficiency	Product
391.4	330	0.25	82.50
427.8	93	0.23	21.39
470.9	17	0.19	3.23
358.2	33	0.23	7.59
423.6	16	0.23	3.68
465.2	4.7	0.20	0.94
Sums	489		119.3

a) Wavelengths and cross-sections measurements at 200 keV are from the literature [1],[2].

We have also checked the relative quantum efficiencies of three PMTs: The XP2020 used for the PS measurements, a spare XP2020, and the EG&G C-942 channel PMT used for the Booster measurements. The measurements were made using the same blue LED as for the acceptance measurements described below. After correcting for the published quantum efficiencies and the active areas of the different PMTs, we found the quantum efficiencies to be equal within 22%, which agrees well with our estimated error of 25%.

The factor k_2 accounts for the single electron events not counted due to the non-zero discriminator threshold. To correct for this effect, for several cases we measured the number of counts as a function of the discriminator threshold. The derivative of this data is another way to measure the SES. By fitting the SES with a Poisson distribution, and analytically integrating the resultant curve to calculate the fraction of missing counts, we determined the correction factor. The corrected number of counts should be independent of the threshold setting, and this is in fact the case, as shown in Table 4. For the case of a 7 mV threshold (a value used in many of our measurements) $k_2 = (1 – 0.12) = 0.88$. We estimate the accuracy of this parameter to be about 7%.

Table 4. Table of correction factors for the non-zero discriminator threshold.

Threshold (mV)	Fraction not counted (=f)	Data set 1 (counts[a])	Corrected (counts[c])	Data set 2 (counts[b])	Corrected (counts[c])
7	0.12	102	116	50	57
10	0.29	79	111	39	55
13	0.48	57	110	29	56

a) 24 GeV/c beam cycle. Number shown is normalized counts, equal to (number of counts) / [(gas pressure in torr) (no. of protons / 10^{10})].
b) 14 GeV/c beam cycle. Number shown is normalized counts, equal to (number of counts) / [(gas pressure in torr) (no. of protons / 10^{10})].
c) Corrected counts is (measured counts) / (1-f).

The correction factor for the light transmission, k_3, depends on the wavelengths of the photons and the material used for the optical windows and lenses. The vacuum windows used in the PS accelerator vacuum tank, and at the entrance to our optical system, are both fused quartz. The first lens is optical quality fused silica, and the remaining three lenses are achromats made from a sandwich of BK7 and either SF5 or SF12 optical glass, coated with an anti-reflective coating. The window at the exit of the optical system is standard glass. The quartz vacuum windows and the fused silica lens were chosen for their radiation-hard properties. The transmission factors for each of these components, taken from manufacturers data, are shown in Table 5. As for the case of the quantum efficiency correction factor k_1, we use the wavelengths and relative intensities from Reference [1],[2] (200 keV). The ratio of the product column sum to the cross-section column sum gives $k_3 = 0.612$. We estimate the accuracy of k_3 to be 15%.

Table 5. Table to compute the transmission correction factor, k_3.

Wavelength (nm)	Cross Sctn (x 10^{-19} cm^2)	Quartz window	Quartz window	Fused Si lens	500 mm lens	1000 mm lens	310 mm lens	Glass window	Product
391.4	330	0.90	0.90	0.93	0.955	0.955	0.955	0.90	194
427.8	93	0.90	0.90	0.93	0.995	0.995	0.995	0.90	62
470.9	17	0.90	0.90	0.93	0.995	0.995	0.995	0.90	11
358.2	33	0.90	0.90	0.93	0.930	0.930	0.930	0.87	17
423.6	16	0.90	0.90	0.93	0.990	0.990	0.990	0.90	10
465.2	4.7	0.90	0.90	0.93	0.995	0.995	0.995	0.90	3
Sums	489								299

The counting time, T_{int}, was typically about 100 ms. This parameter is controlled to an accuracy of better than 1%.

Data analysis – acceptance of the optical system

We measured the optical system acceptance, A, after removing the optical system from the PS beam tunnel at the completion of the year 2000 run. We used a blue LED mounted in a 2 x 2 x 2 cm^3 Teflon block, with a 1 mm diameter hole in front of the LED to simulate an isotropic light source. The source was mounted on a translation table placed inside a mock-up of the vacuum tank used in the PS beam line. The translation table allowed us to perform measurements at all the possible emission points along the path of the beam. A 1 mA current in the LED produced sufficient light to give good counting statistics without saturating the electronics.

We first measured the count rate with the XP2020 PMT placed 164 mm (approximately equal to the distance between the beam and the vacuum tank view port) from the LED. Next we measured the count rate with the PMT at the focal point of the optical system exit. The ratio of the two measurements is the ratio of the optical acceptances:

$$\frac{Acceptance_{OS}}{Acceptance_{PMT}} = 0.027 \ .$$

We can easily calculate the acceptance of the PMT measurement given the 20 mm radius active area the PMT:

$$Acceptance_{PMT} = \frac{1}{2}\left\{1-\cos\left[\operatorname{atan}\left(\frac{20\ \mathrm{mm}}{164\ \mathrm{mm}}\right)\right]\right\} = 3.7\cdot 10^{-3} \ .$$

The acceptance of the optical system is then

$$Acceptance_{OS} = Acceptance_{PMT}\cdot\frac{Acceptance_{OS}}{Acceptance_{PMT}} = 3.7\cdot 10^{-3}\cdot 0.027 = 9.9\cdot 10^{-5} \ .$$

We also measured the acceptance of the optical system as a function of LED position, i.e., the vignetting factor. The position was varied ±30 mm to include the entire acceptance range. We found the average value to be 69% of the value with the LED at the center position.

The above measurement was made with a blue LED with a wavelength of about 400 nm – close to the wavelength of the strongest N_2 cross-section. It is useful to define the acceptance to not include the dependence on wavelength. This will allow us to more easily include the wavelength-dependent attenuation for any given combination of wavelengths, and also allow a more straightforward comparison with optical modeling codes. From Table 5 we see that the windows and lenses in our optical system attenuate 391 nm light by a factor of 0.59. The total acceptance, A, of the optical system is then (0.69)(9.9×10^{-5})/(0.59) = 1.2×10^{-4}. We estimate the error of this measurement to be about 20%.

Since the acceptance is such a crucial parameter in the cross-section measurement we also computed it using the optical modeling code ZEMAX[9]. This code includes factors such as effective apertures and vignetting, but not wavelength-dependent attenuation. Using the lens parameters taken directly from the manufacturer's data, we computed an acceptance of 3.54×10^{-4}, an active length L of 6 cm, and a vignetting factor of 0.523. The factor A is the product of 3.54×10^{-4} and 0.523, or 1.85×10^{-4}. Modern optical codes such as ZEMAX are quite accurate. The calculated focal points and magnification factors were in good agreement with our measurements. We estimate the accuracy of the code to be about 20% for the combination of the acceptance, the optical length, and the vignetting factors.

The measured and calculated acceptances, agree within the estimated errors of ±20%. For the cross-section calculations we shall take the mean, or $A = 1.5 \times 10^{-4}$ ±20%.

The horizontal and vertical extent of the beam is well within ±1 cm of the beam line center. We used ZEMAX to compute the effect of displacing the line source 1 cm horizontally (i.e. closer to or further from the vacuum tank window), vertically, or both. These effects result in at most a 9% reduction in the vignetting factor. The overall error in the acceptance of the optical system is then about 20% + 9% = 29%

Cross-section results

Cross-section measurements were made at 2.1, 14, 24, and 26 GeV/c in the PS. For each momentum, the data-collection system counted the number of pulses from the PMT/discriminator and simultaneously recorded the beam intensity and the gas pressure. To improve the statistical accuracy, the number of counts from several (typically six) PS cycles were added together. A sample of our data is shown in Table 6. To check that the number of photons counted scaled with the gas pressure, data were taken for a range of gas pressures. An example of one demonstration of the expected linearity is shown in Figure 3. Our measured cross-sections are shown in Table 7 and Figure 4. These are of course the total cross-sections for all the individual excited states that emit light in the wavelength range to which our detector is sensitive. The figure shows all our measurements, to give an appreciation of the spread in repeated measurements (see error discussion below), while the table shows the average for each beam momentum. The 2.1 GeV/c point (PS injection momentum) is used to normalize the booster measurements where 2.1 GeV/c (1.4 GeV) corresponds to the extraction momentum.

Table 6. Counts for N_2 gas example per 10^{10} protons in the beam.

Beam momentum (GeV/c)	Gas pressure (torr)	*BGO*	*BGC*	*BNO*	*BNC*
2.1	1.8×10^{-6}	100	10	23	10
14	2.0×10^{-6}	128	34	16	12
24	1.9×10^{-6}	128	3	17	2
26	2.0×10^{-6}	129	2	16	2

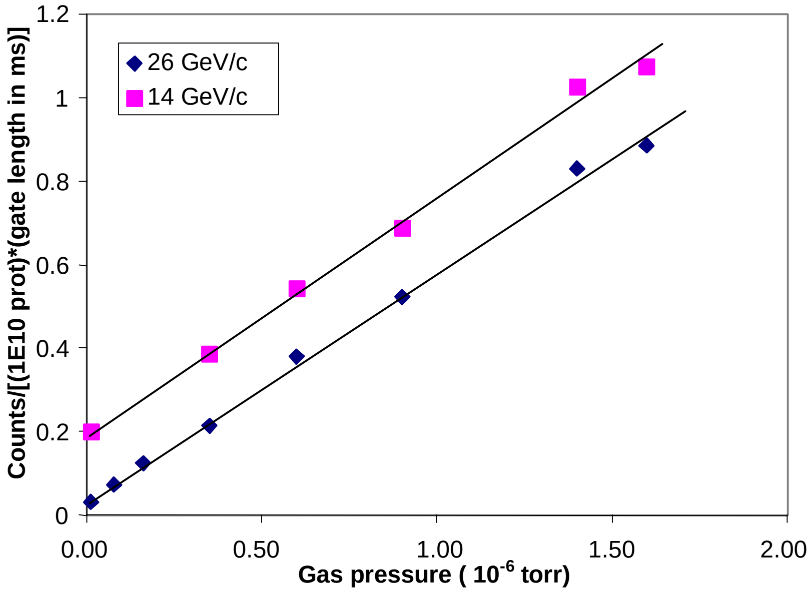

Figure 3. Count rate vs. N_2 gas pressure for two different PS beam cycles. Note the large background contribution for the 14 GeV/c case.

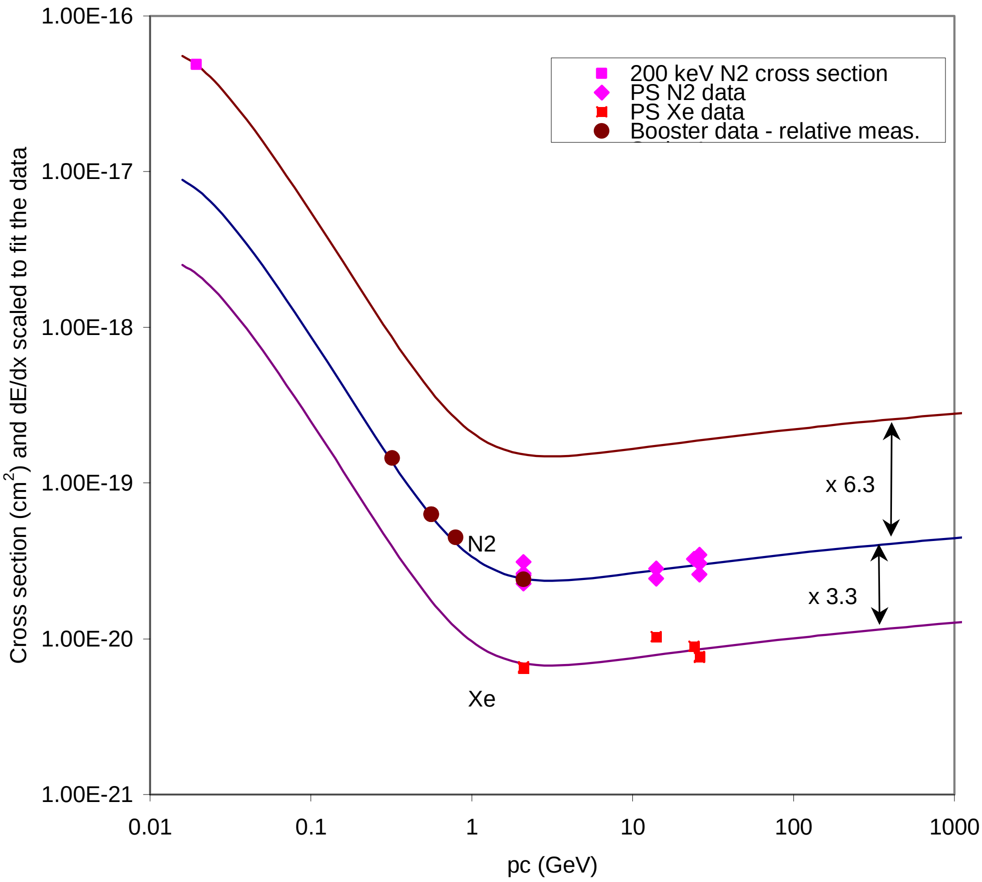

Figure 4. Measured cross-sections for N_2 and Xe. Solid lines are the Bethe-Bloch stopping powers, scaled to pass through the data.

Table 7. Cross-section measurements.

Beam Momentum (GeV/c)	N_2 measured[a] cross-section (x 10^{-20} cm^2).	Xe measured[b] cross-section (x 10^{-20} cm^2)
2.1	2.6	0.65
14	2.6	1.0
24	3.3	0.90
26	2.9	0.77

[a] Total estimated error is 45%.
[b] Total estimated error is 70%.

One expects that the energy dependence of the gas scintillation cross-sections will scale with the dE/dx Bethe-Bloch stopping power formula [12]. Also shown in Figure 4 is the total of the cross-sections from the 200 keV (p = 19.4 MeV/c) data (see Table 3). If we scale the dE/dx curve to pass through this point, we can extrapolate to our energy range and predict the sum of our cross-sections. The resultant curve is shown in the figure. It lies a factor of 6.3 above the same dE/dx curve scaled to pass through our data points. We conclude that our cross-sections are 6.3 times lower than predicted from dE/dx scaling of the 200 keV data. It is remarkable that the cross-sections scale so well over three decades of incident proton momenta and cross-section values. In the figure we also plot the Xe cross-sections. We applied the same factors to the Xe data as to the N_2 data to compute the absolute Xe cross-sections. This is not completely correct, since the transmission and photocathode quantum efficiency correction factors, k_1 and k_3, assume knowledge of the relative cross-sections at some other energy, which to the best of our knowledge have never been measured. However, by using the same factors we can more easily compare the count rates expected in gas scintillation beam diagnostic systems.

It is sometimes useful to express the photon production in terms of energy loss. Taking the N_2 data point measured at 2.1 GeV/c (since this scales with the stopping power, it is equally valid for other energies), where the Bethe-Bloch formula gives dE/dx = 1.88 MeV-cm^2/gm for N_2 gas, we find that there is 3.4 keV energy loss per photon created in the visible range. Visible photon creation is therefore much less efficient when compared to, for example, gas ionization, which requires only about 35 eV of energy loss to produce an electron – ion pair.

For the case of Xe, where the cross-section at 2.1 GeV/c is 6.5 x 10^{-21} cm^2, and dE/dx = 1.28 MeV-cm^2/gm, we find there is 43 keV of energy loss per photon created in the visible range.

Error analysis

The error analysis can be divided into two main categories – experimental and systematic. The experimental error is related to the statistical uncertainties caused by low numbers of counts, errors in background subtraction, and other errors associated with determining how many counts are due to gas scintillation photons. The systematic error is common to the entire data set, and is a measure of the uncertainty in the determining the absolute cross-section from the data.

Since this is a counting experiment, the statistical error on the number of counts, ε_N, is just $\sqrt{N}$. The gas scintillation photon signal, from above, is

$$P_s = (BGO - BGC) - (BNO - BNC).$$

Assuming the counts due to gas scintillation and the counts due to the background are uncorrelated, the statistical error in P_s is simply

$$\varepsilon_{P_s} = \left[\left(\frac{\partial P_s}{\partial BGO} \right)^2 \varepsilon_{BGO}^2 + \left(\frac{\partial P_s}{\partial BGC} \right)^2 \varepsilon_{BGC}^2 + \left(\frac{\partial P_s}{\partial BNO} \right)^2 \varepsilon_{BNO}^2 + \left(\frac{\partial P_s}{\partial BNC} \right)^2 \varepsilon_{BNC}^2 \right]^{1/2}$$

$$= \sqrt{BGO + BGC + BNO + BNC} \, ,$$

where *BGO*, *BGC*, *BNO*, and *BNC* are the counts collected for the cases of beam on, gas on, shutter open; beam on, gas on, shutter closed; beam on, no gas, shutter open; and beam on, no gas, shutter closed. We typically acquire several thousand counts due to gas scintillation, so the statistical error computed in this way is less than one percent. However, the spread in the data for repeated measurements at the same proton energy is much greater than one percent. This indicates that the local error is due to more than just statistics, and that it is dominated by the other error sources. By examining the spread in the cross-sections made by repeating the measurements under a variety of beam conditions (different gas pressures, different beam cycles, different beam losses, etc.), we can get a more realistic estimate of the error. The largest spread in the data occurs in the 26 GeV/c measurements, where the standard deviation is 15% of the mean. We therefore conclude that a more realistic estimate of the experimental error is ±15%.

To estimate the systematic error, we must determine the accuracy of the parameters needed to transform the measurement of the number of counts into a cross-section. These parameters are the gas density, ρ; the proton flux, *F*; the active length of the optical system, *L*, the acceptance of the optical system, *A*; the PMT quantum efficiency, k_1; the discriminator threshold correction factor, k_2; the light transmission through the optical system, k_3; and the counting time interval, T_{int}. Each of these parameters enter the cross-section calculation as an uncorrelated multiplicative factor, so the rms total error is just the individual errors added in quadrature. Using the error estimates in the above discussion, the rms systematic error is then

$$\varepsilon_{syst} = \left[\varepsilon_\rho^2 + \varepsilon_F^2 + \varepsilon_{l+A}^2 + \varepsilon_{k_1}^2 + \varepsilon_{k_2}^2 + \varepsilon_{k_3}^2 + \varepsilon_{T_{\mathrm{int}}}^2 \right]^{1/2}$$

$$= \left[0.04^2 + 0.01^2 + 0.29^2 + 0.25^2 + 0.07^2 + 0.15^2 + 0.01^2 \right]^{1/2} = 0.42$$

To get the total error, we add the experimental (15%) and the systematic (42%) errors in quadrature. The total error on the absolute N_2 cross-section is then 45%. We estimate the total error on the Xe cross-section to be 25% above this since we used the k_1 and k_3 correction factors appropriate for N_2 in the Xe cross-section calculation.

Spectral measurements

As discussed earlier, the PS experimental setup contained a remote-controlled nine-position wheel located directly in front of the PMT, which allowed filters and optical blinds to be rotated into place. We used one position for an optical blind (4 mm thick aluminum) to measure the background, and seven positions for 40-nm bandwidth optical interference filters [13] for coarse spectral measurements. The last position was left open for the full cross-section measurement. Figure 5 and Figure 6 show the spectral measurements using the filters. Also shown are the filter transmission curves and the response of the PMT photocathode. The N_2 spectrum shows that most of the strength is concentrated in the 388 – 427 nm range, as expected from earlier N_2 cross-section measurements. The Xe spectrum is broadband and quite flat after accounting for the response of the photocathode.

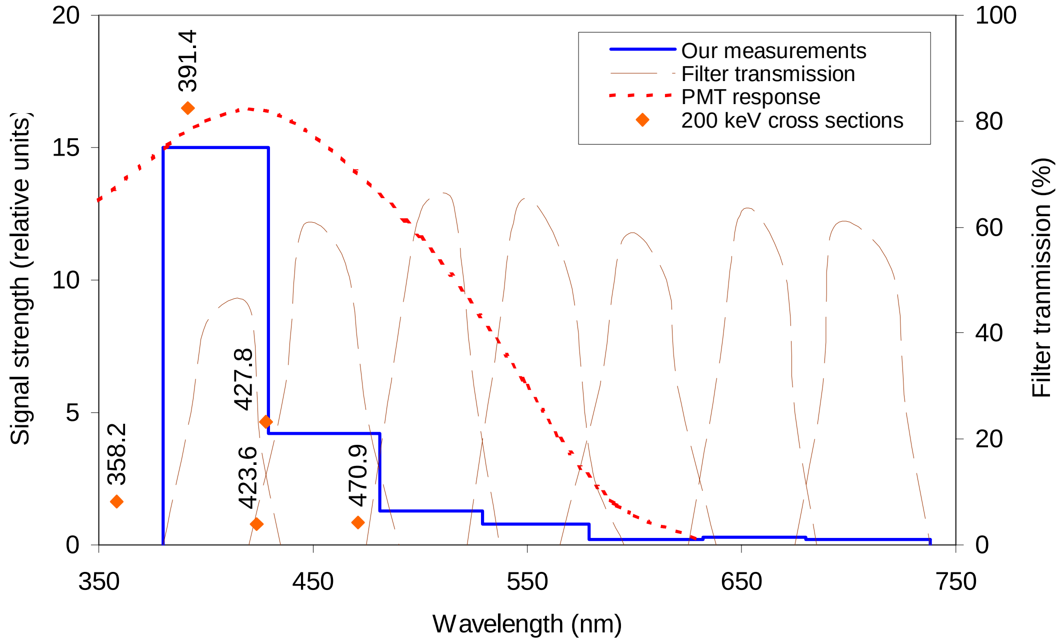

Figure 5. N_2 spectral measurements. Solid line: signal strength for the seven different filters; long-dash line: transmission as a function of wavelength for the filters; dotted line: response of the PMT photocathode; diamonds: relative signal strengths of the N_2 cross-sections measured at 200 keV.

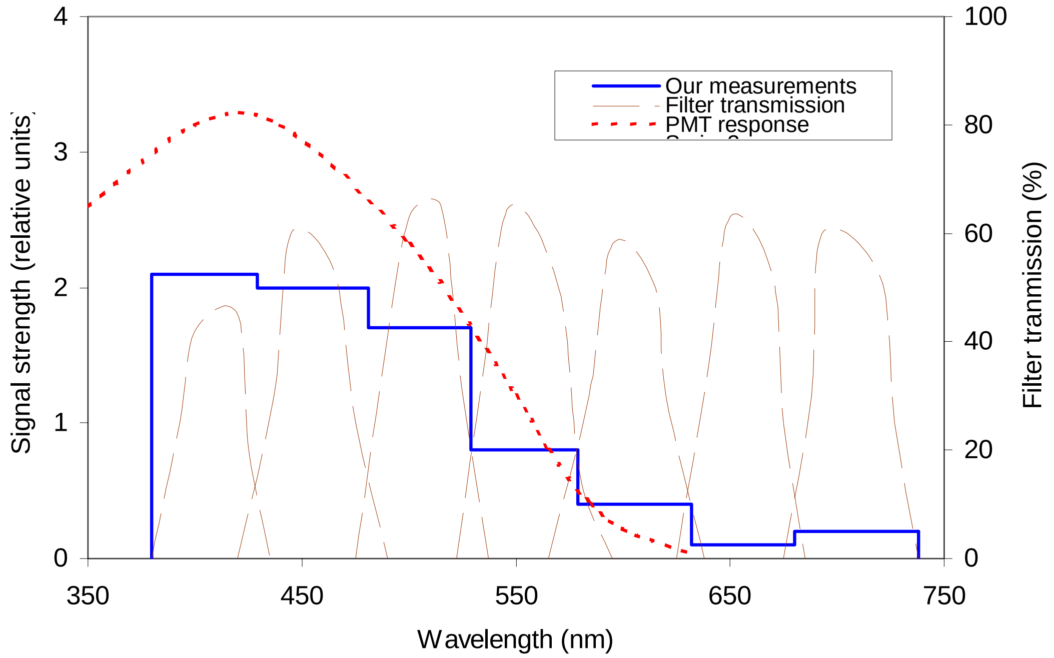

Figure 6. Xe spectral measurements. Solid line: signal strength for the seven different filters; long-dash line: transmission as a function of wavelength for the filters; dotted line: response of the PMT photocathode.

Excited State Lifetimes

The excited state lifetimes are important parameters in the design of a beam profile monitor system. Movement of a gas molecule away from the point where it interacted with the beam translates to an inaccuracy in the profile measurement. The longer the lifetime, the greater the inaccuracy.

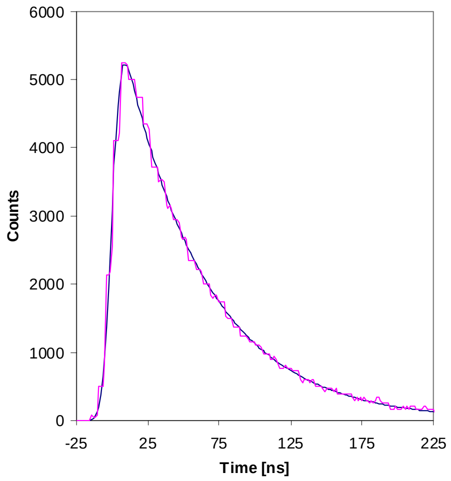

Figure 7. N_2 lifetime, no optical filter.

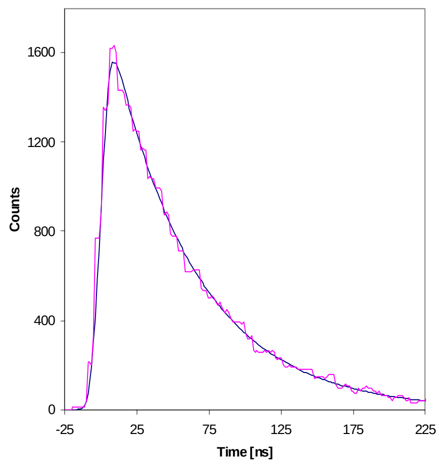

Figure 8. N_2 lifetime, 388 – 427 nm optical filter.

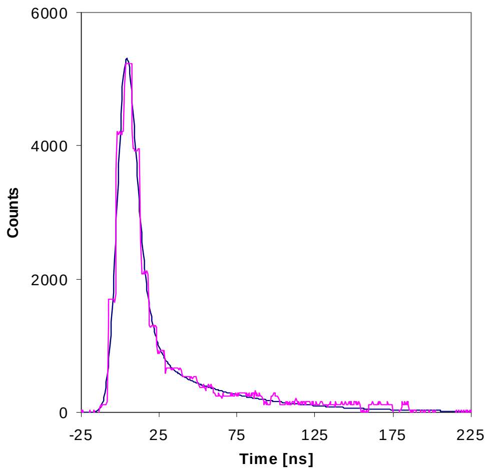

Figure 9. Xe lifetime measurement, no optical filter.

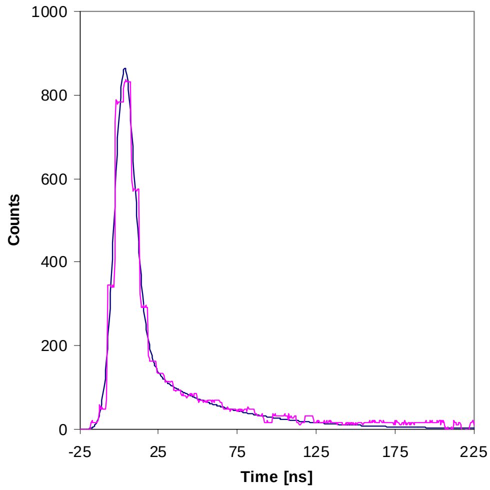

Figure 10. Xe lifetime measurement, 388 – 427 nm optical filter.

To measure the lifetimes of the excited states, the PS was specially set up for a single short bunch (σ_s ~5 ns) at 26 GeV/c. The PMT low-level discriminator (set for the optimum value of 7 mV) was used to start a Time to Analog Converter (TAC). We derived the TAC stop signal from a signal locked to the PS revolution frequency. In this way the amplitude of the output pulse of the TAC is proportional to the delay between the bunch crossing and the photon emission. Starting the TAC on the photon signal rather than the bunch crossing minimizes the false starts (starts with no stop). During our lifetime measurements, the maximum count rate was of the order of one photon per 11 bunch revolutions. This rate is so small that the probability of missing some photons, and thus distort the lifetime measurement, is negligible (a photon that arrives on the detector after the start signal has already been triggered cannot be detected and is thus missed.)

We used a LeCroy Multi-Channel Analyzer (MCA) to collect the TAC output pulses, and a digital oscilloscope to display the MCA output. The oscilloscope output was then read out by a computer, and the results were analyzed off line. A simple reversal of the multi channel analyzer (MCA) horizontal axis produces the familiar lifetime plots shown in Figure 7 to Figure 10. We made lifetime measurements with and without optical filters in front of the PMT. Although we measured the lifetime spectra for six different filter bandwidths, we present the results of just the filter with the highest transmission. The other filters had lower count rates and lower signal to noise ratios, and the results were qualitatively the same as the highest-transmission filter.

The analytical expression of the distribution function is given by the convolution of the gaussian bunch shape and the exponential decay of the excited states. Assuming a single time constant,

$$F(t) = \frac{C}{\tau\sqrt{\sigma}} \int_{-\infty}^{t} e^{-z^2/2\sigma_s^2} e^{-(t-z)/\tau} dz$$

Or, for the case of two time constants,

$$F(t) = \frac{1}{\sqrt{\sigma}} \int_{-\infty}^{t} e^{-z^2/2\sigma_s^2} \left(\frac{C_1}{\tau_1} e^{-(t-z)/\tau_1} + \frac{C_2}{\tau_2} e^{-(t-z)/\tau_2} \right) dz$$

where C is a normalization constant, σ_s is the bunch length and τ is the lifetime of the excited state. We performed a minimization fit on the data to extract the parameters. To obtain a meaningful fit we must estimate the errors on the data points.

The first error component is due to the statistical fluctuation of the counts in a given channel and can thus be expressed as $\sqrt{N}$, where N is the number of counts for that particular channel. Since we used a digital oscilloscope to acquire the MCA output, two additional error components arise. The first is given by the limited resolution of the 8 bit digitization and can be expressed as the rms of a square distribution whose width is given by the oscilloscope resolution times the scaling factor (Counts/Volt). The second component is caused by the oversampling of every channel. In fact the scope acquires many more points than the number of channels in the histogram (there are an average of 3.5 data points for every channel). The result is a fit to a staircase profile with a smooth function. This error can be considered as an uncertainty on the x scale (time) equal to the width of one channel. The error component is equal to the rms of a square distribution whose width is the product of the slope of the function times the time width of one channel of the histogram. After these error estimates are included in the fitting routine we obtain the results shown in Table 8 and Table 9.

Table 8. N_2 lifetime measurement fit parameters.

	No filter	388 – 427 nm filter
Bunch length (σ_s)	5.4 ± 0.2 ns	5.3 ± 0.2 ns
Time constant (τ)	57.7 ± 0.2 ns	58.7 ± 0.3 ns
χ^2 / degree of freedom	1.4	1.3

Table 9. Xe lifetime measurement fit parameters.

	No filter	388 – 427 nm filter
Bunch length (σ_s)	5.09 ± 0.05 ns	5.78 ± 0.07ns
Amplitude 1 (C_1)	43.4 ± 0.4	6.43 ± 0.08
Amplitude 2 (C_2)	32.4 ± 0.3	5.16 ± 0.07
Time constant 1 (τ_1)	6.0 ± 0.1 ns	3.8 ± 0.1 ns
Time constant 2 (τ_2)	51.5 ± 0.9 ns	49.0 ± 1.1 ns
χ^2 / degree of freedom	5.4	2.1

The fit errors listed in the tables represent the fit error only. They do not include the error on the scaling factor used to compute the time from the MCA channel number, which we estimate to be about 3%. We obtained the scaling factor between the oscilloscope time base and the actual decay time of the molecule in two parallel ways, each resulting in an error of about 3%. The first method was to compare the longest acquired time with the revolution period, and the second method was to introduce a known delay in the TAC start signal and observe the shift of the spectrum. Previous work [3] at 400 keV on N_2 lifetimes resulted in highly accurate lifetime measurements of 60.4 ± 0.4 ns. Given the larger overall error of 3% on our lifetime measurement of 57.7 ns, our N_2 results are consistent with the 400 keV measurements.

To the best of our knowledge, scintillation lifetime measurements have never been made for Xe gas. We found our data to be well described using two different lifetimes – one strong component with a 6 ns lifetime, and a weaker component with a 52 ns lifetime. We observed slightly shorter lifetimes with a narrowband filter to select the strongest states. In this sense Xe is a better gas to use for gas scintillation profile measurements.

Once the lifetimes have been measured, the next step is to determine how far the excited gas particle can move away from the point where it interacted with the beam. Three components contribute to this motion: thermal motion, momentum exchange from the beam-gas excitation interaction, and interactions of the excited molecule with the electromagnetic field of the beam.

From the kinetic theory of gases, the rms velocity of a gas particle is [14]

$$v_{therm} = \sqrt{\frac{2k_B T}{M}}\ ,$$

where k_B = 1.38 x 10^{-23} joule/°K is Boltzmann's constant, T is the temperature, and M is the mass of the gas molecule. Lighter molecules have higher velocities, so N_2 is worse than Xe, and we will use the N_2 mass in our calculation. The temperature is 293 °K. Inserting the numbers gives

$$v_{therm} = 4.2\cdot 10^{-4}\ \text{mm/ns}.$$

Little is known about motion imparted to gas molecules due to beam interactions [15]. In a measurement with a 50 MeV proton beam incident on air at 1 x 10^{-6} torr, DeLuca [16] concluded that the total resultant kinetic energy was 0.014 eV. This includes the contributions from thermal, electromagnetic, and momentum exchange. For N_2 gas, 0.014 eV corresponds to a velocity of

$$v_{exch} = \sqrt{2\cdot\frac{0.014\ \text{eV}}{M}} = 3.1\cdot 10^{-4}\ \text{mm/ns}\ \ ,$$

even less than the thermal velocity. We conclude that momentum exchange results in a small contribution, but since it is a poorly understood phenomenon, to be conservative, we shall double the results of DeLuca's measurement and assume that it is entirely due to momentum exchange.

The electromagnetic forces from the beam are predominantly electric. The relevant beam parameters are the transverse dimensions and the beam current. For a beam of current I, velocity β, and transverse dimensions σ_x and σ_y, the electric field (in, for example, the x direction) is

$$E_x(x', y') = \frac{I}{4\pi^2 \varepsilon_0 \beta c \sigma_{x'} \sigma_{y'}} \int dx \int dy\, e^{-\frac{x^2}{2\sigma_x^2}} e^{-\frac{y^2}{2\sigma_y^2}} \frac{x' - x}{(x-x')^2 + (y-y')^2}$$

When the PS ring is accelerating beam for the LHC, there will be 84 bunches 3.8 ns long, spaced by 25 ns, with up to $1.7 \cdot 10^{11}$ protons per bunch. The minimum transverse dimensions of the bunch are expected to be σ_x = 2.1 mm and σ_y = 1.1 mm when the momentum spread $\Delta p/p$ is $5 \cdot 10^{-4}$. For this case, the maximum electric field is $1.3 \cdot 10^5$ V/m. If the gas molecule has a charge of +1, as for the case of N_2^+,

$$v_{beam} = \frac{E\,q\,t}{M} = \frac{(1.3 \cdot 10^5 \text{ V/m})(1.6 \cdot 10^{-19} \text{coul})(3.8 \text{ ns})}{4.68 \cdot 10^{-26} \text{ kg}} = 1.7 \cdot 10^{-3} \text{ mm/ns}$$

Of course if the particle emitting the photon is neutral it will be unaffected by the beam's electric field. In this sense N_2 is less than ideal. In general, several bunches may pass by before the photon is emitted, and each time the velocity could increase. The distance traveled will be

$$d_{beam} = \sum_{n=1}^{\text{int}(\tau/T)+1} n\, v_{beam} \min(T, \tau-(n-1)T) \;\; ,$$

where τ is the lifetime of the excited molecule, int(*a/b*) is the integer portion of the quantity *a/b*, and min(*a,b*) is the minimum of *a* or *b*.

For example, for a bunch spacing of time T = 25 ns, v_{beam} = 1.7 μm/ns, and a photon emitted after τ = 60 ns, the distance traveled will be

$$(v_{beam}\text{T}) + (2v_{beam}\text{T}) + (3v_{beam} \cdot 10 \text{ ns}) = 0.179 \text{ mm.}$$

To get the total rms distance traveled we add the pieces in quadrature:

$$d_{rms} = \left[(v_{therm}\tau)^2 + (v_{exch}\tau)^2 + d_{beam}^2\right]^{1/2}$$

Considering our present case of N_2^+ gas,

$$d_{rms} = \left[\left(4.2 \cdot 10^{-4} \text{ mm/ns} \cdot 60 \text{ ns}\right)^2 + (3.1 \cdot 10^{-4} \text{ mm/ns} \cdot 60 \text{ ns})^2 + (0.179 \text{ mm})^2\right]^{1/2}$$

$$= 0.18 \text{ mm}.$$

The dominant contribution to the reduction in resolution is the beam's electric field. If the excited gas molecule is neutral, however, this contribution would be absent, and the particle would move only about a tenth of the distance.

Conclusions

We have measured absolute gas scintillation cross-sections for visible lines in N_2 and Xe gas over the 1.4 to 25 GeV proton energy range. We have also measured relative cross-sections between 0.05 to 1.4 GeV. Within our data set the results are in good agreement with dE/dx scaling. When compared to extrapolations from measurements made at 200 keV proton energy, the N_2 cross-sections are about 6.3 times lower than predicted. The Xe cross-sections are about 3 times lower than the N_2.

The N_2 lifetime measurements are consistent with earlier measurements made at 400 keV proton energy – a single 60 ns lifetime. The lifetimes using a narrow band filter are not shorter. The Xe lifetimes show at least two components. With no filter, the two components have lifetimes of 6.0 and 51.5 ns. Using the filter with the highest transmission (388 – 427 nm), the lifetimes reduce slightly to 3.8 and 49.0 ns. The long lifetime states are populated 20 to 25% less often than the short lifetime states.

The N_2 spectral measurements show the majority of the strength between 385 and 430 nm, as expected from the 200 keV measurements. The Xe spectral measurements show strength that is broad band over the range of our measurements, from about 385 to about 600 nm.

The gas scintillation cross-sections in the proton energy range above about 1 GeV, while quite weak, are nevertheless sufficiently strong to be used for beam diagnostics instrumentation in accelerators with large beam currents. Background signals due to beam loss are also an important factor, and these must be carefully accounted for in beam diagnostic system designs.

Acknowledgements
Thanks to Heribert Koziol for supporting this work, to Hallgeir Klette and the vacuum crew for all their help with the gas injection systems, and to Alessandro Variola for his help in the design of the optical system.

---

[1] R.H. Hughes, J.L. Philpot, and C.Y. Fan, "Spectra Induced by 200-kev Proton Impact on Nitrogen", Phys Rev. 123 (1961) 2084.

[2] J.L. Philpot and R.H. Hughes, "Spectroscopic Study of Controlled Proton Impact on Molecular Nitrogen", Phys. Rev. 133 (1964) A107.

[3] L.W. Dotchin, E.L. Chupp, and D.J. Pegg, "Radiative lifetimes and pressure dependence of the relaxation rates of some vibronic levels in N_2^+, N_2, CO^+ and CO*", Journal Of Chem. Physics, 59 (1973) 3960.

[4] G. Burtin, J. Camas, G. Ferioli, R. Jung, J. Koopman, R. Perret, A. Variola, J.M. Vouillot, "The Luminescence Profile Monitor of the CERN SPS", Proceedings of the 2000 European Particle Accelerator Conference, Vienna, 26-30 June 2000.

[5] F. Kakimoto, C. Loh E., M. Nagano, H. Okuno, M. Teshima and S. Ueno, "A measurement of the air fluorescence yield", Nucl. Inst. And Meth. A372 (1996) 527-533.

[6] E. Jones, R. Kofler and P. Strolin, "Optical determination of ISR luminosity", CERN report CERN-ISR-VA-73-57.

[7] P. Actis, T. Dorenbos, C. Johnson, "An Optically Coupled Differential Beam Time Structure Monitor for Slow Extraction", CERN note PS/CCI/Note 76-7.

[8] M. Mutterer, J.P. Theobald and K.-P. Schelhaas, "A Low-Pressure Noble-Gas Scintillation Counter for Havy-Ion Detection", Nucl. Instr. and Meth 144 (1977) 159-166.

[9] ZEMAX optical modeling code, Focus Software, Tucson, AZ, USA.

[10] Hallgeir Klette, CERN, private communication, April 2000.

[11] Patrick Odier, CERN, private communication, May 2000.
[12] See, for example, the Review of Particle Physics, Eur. Phys. J. C 15 (2000) 1.

[13] Melles-Griot interference filter set, product number 03 IFS 008.

[14] L.L. Marton et. al., Methods of Experimental Physics – v. 14 Vacuum Physics and Technology, ed., New York Academic Press (1979).

[15] F. Hornstra, “A Beam induced Gas Scintillation Profile Monitor for HERA”, Internal Report DESY HERA 89-04.

[16] W.H. DeLuca, “Beam Detection Using Residual Gas Ionization”, IEEE Trans. Nucl. Sci. NS-16 (1969) 813.